CHEMICAL PHYSICS

In silico construction of a flexibility-based DNA Brownian ratchet for directional nanoparticle delivery

Suehyun Park*, Jeongeun Song, Jun Soo Kim†

Brownian particles confined in a system with periodic and asymmetric potential can be transported in a specific direction along the potential by repetitively switching the potential on and off. Here, we propose a DNA-based Brownian ratchet for directional transport of positively charged nanoparticles in which nanoparticle delivery follows the path dictated by a single, long, double-stranded DNA. We performed Brownian dynamics simulations to prove its realization using coarse-grained models. A periodic and asymmetric potential for nanoparticle binding is constructed along a single, long, double-stranded DNA molecule by a novel strategy that uses variation in sequence-dependent DNA flexibility. Directional and processive motion of nanoparticles is achieved by changing salt concentration repetitively over several cycles to switch the asymmetric potential on and off. This work suggests that double-stranded DNA molecules with elaborately designed flexibility variation can be used as a molecule-scale guide for spatial and dynamic control of nanoparticles for future applications.

INTRODUCTION

The migration of particles in solution is controlled in a specific direction, conventionally, by applying external fields including magnetic, electric, thermal, and concentration fields that bias the particle motion. In recent years, more sophisticated strategies based on a Brownian ratchet process have been developed for directional transport and sorting of Brownian particles in the absence of any external bias (*1*–*14*). In a type of Brownian ratchet mechanism called on-off ratchet, for example, Brownian particles confined in a system with a periodic and asymmetric potential are transported in a specific direction along the potential by repetitively switching the potential on and off (*1*–*7*, *13*). In earlier Brownian ratchets, asymmetry in potential was obtained typically by using optical (*6*, *10*, *13*) or dielectrophoretic (*5*, *8*, *11*) forces. However, they are insufficient to manipulate particles of nanometer scale. Therefore, their use was limited to the transport of micrometer-sized particles, with only a few exceptions (*7*, *14*). In addition, particle motion in other directions perpendicular to the potential is limited by the scale of particle confinement, typically micrometers, making it difficult to have precise control of particle localization in a three-dimensional space.

Here, we propose a DNA-based on-off Brownian ratchet for directional transport of positively charged nanoparticles (NPs) and prove the realization by performing Brownian dynamics (BD) simulations of coarse-grained models of a single, long, double-stranded DNA (dsDNA) molecule and a positively charged NP of 4 nm in diameter. An asymmetric potential for DNA-NP binding is constructed along a dsDNA fragment containing 384 base pairs corresponding to 130 nm in length such that the local flexibility of the base pair sequence is increased gradually along the fragment at physiological salt concentration as shown in Fig. 1 (A and B). The fragment is repeated so that the asymmetric potential is repeated periodically along a single, long, dsDNA molecule with several hundreds or thousands of base pairs, as shown in Fig. 2A. Directional and processive motion of an NP is achieved in a specific direction along the dsDNA by changing the salt concentration repetitively over several cycles (Fig. 2C) to switch the asymmetric potential on and off (Fig. 2, A and B). Since an NP does not dissociate from dsDNA at the concentrations under investigation, the conformation of a single dsDNA molecule dictates the path along which NPs are processively delivered, resulting in a precise control of NP localization from one end to the other along a dsDNA. The transport distance can reach several hundreds or thousands of nanometers along a dsDNA by synthesizing the dsDNA with repeated sequences of flexibility gradient and anchoring its two ends at two distant substrates (*15*).

The novelty of this DNA-based Brownian ratchet is in the use of variation in sequence-dependent dsDNA flexibility in addition to the construction of a periodic and asymmetric potential along a single dsDNA molecule. With increasing capability for precise DNA synthesis with specific base pair sequences (*16*), there are rapid developments in the field of DNA nanotechnology, including two- and three-dimensional structural assemblies of DNA molecules (*17*, *18*), DNA-templated formation and control of nanoscale structures (*15*, *19*), and construction of programmable DNA machines (*20*–*22*). In most of these developments, sequence-specific hybridization of complementary DNA strands has been used as an essential tool for connecting and exchanging different DNA strands. However, sequence-dependent variation of dsDNA flexibility has rarely been exploited. Although dsDNA is very rigid with an average persistence length of $l_p \sim 50$ nm (a measure of rigidity or flexibility), it has been shown that local persistence length (l'_p, inversely proportional to local flexibility) varies with base pair sequences (*23*, *24*). For instance, the local persistence length l'_p of dinucleotide steps ranges from 40 to 55 nm in a sequence-dependent manner (*23*). It was also shown that the persistence length of human DNA segments increases significantly with increasing GC content (*24*). The difference in local persistence length (or local flexibility) may not result in a huge structural difference in dsDNA molecules with several hundreds or thousands of base pairs. Thus, sequence-dependent flexibility variation may not be useful by itself. However, when dsDNA has to be bent by binding with positively charged NPs, the effect of variation in sequence-dependent DNA flexibility can be augmented substantially (*25*) so that it can be used in our DNA-based Brownian ratchet.

Particle delivery along a designated path proposed in this work is already familiar to biologists who study biological motors such as kinesin and myosin, the well-known examples of microscopic

Department of Chemistry and Nanoscience, Ewha Womans University, Seoul 03760, Republic of Korea.
*Present address: School of Chemistry and Biochemistry, Georgia Institute of Technology, Atlanta, GA 30332-0400, USA.
†Corresponding author. Email: jkim@ewha.ac.kr

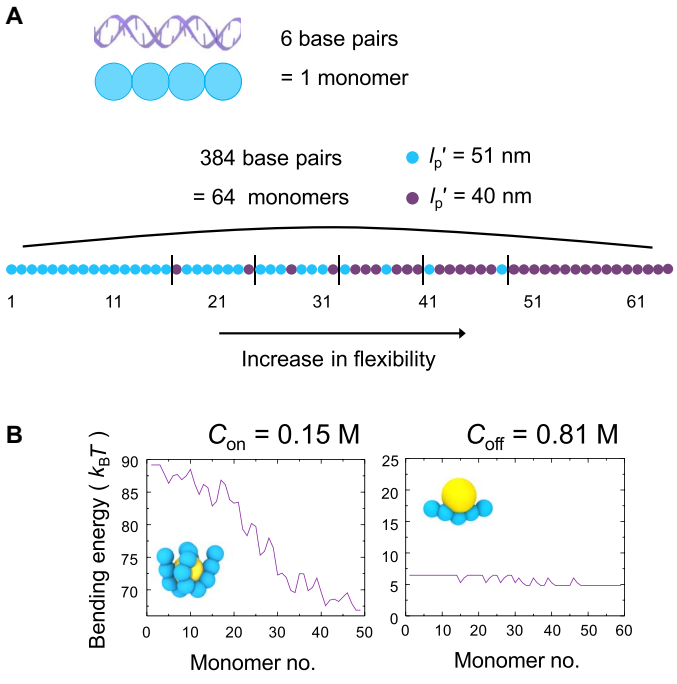

Fig. 1. A DNA fragment with flexibility gradient. (**A**) Model of dsDNA represented by a semiflexible chain of monomers, each of which models a group of 6 DNA base pairs. A dsDNA fragment with flexibility gradient is modeled by a chain of 64 monomers. The local persistence length (l_p') is set for each monomer at either 51 or 40 nm. The sequence-dependent dsDNA flexibility is gradually increased by increasing the fraction of monomers with l_p' = 40 nm. (**B**) Bending energy of dsDNA fragment when it binds with a positively charged NP at solution salt concentrations of C_{on} = 0.15 M and C_{off} = 0.81 M. The bending energy is calculated for a specific, representative conformation of the DNA-NP complex as shown in the inset of each figure along the flexibility gradient of 64-mer dsDNA presented in (A). The monomer number in the *x* axis represents the identity of the first DNA monomer bound to the NP.

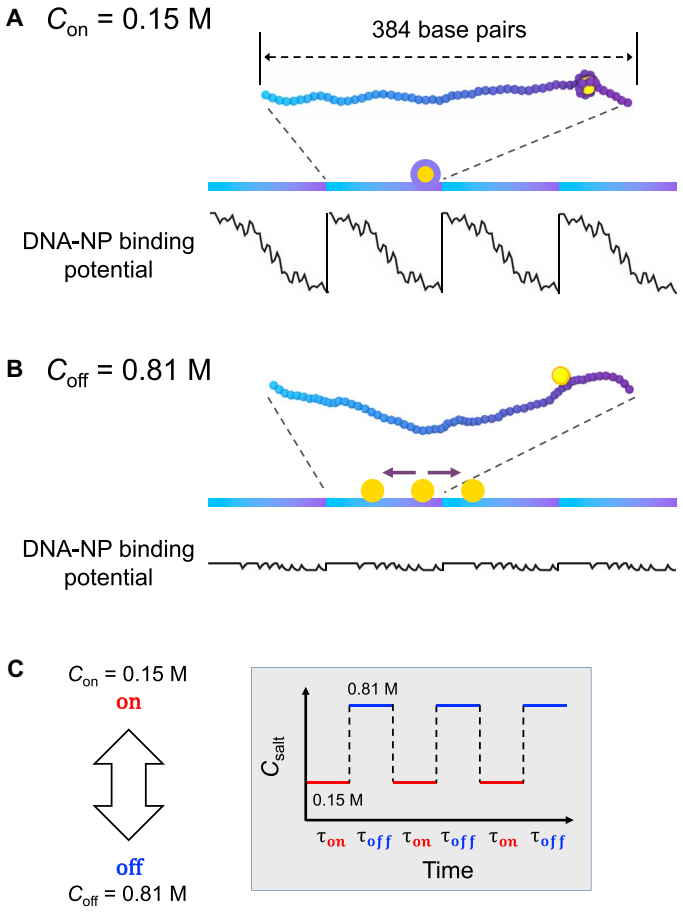

Fig. 2. Construction of a DNA-based Brownian ratchet. (**A** and **B**) Long dsDNA containing four repeat fragments with the flexibility gradient, together with its DNA-NP binding potential energy along the entire dsDNA molecule at solution salt concentrations of C_{on} = 0.15 M and C_{off} = 0.81M, respectively. (**C**) Solution salt concentrations are changed repeatedly between C_{on} = 0.15 M and C_{off} = 0.81 M to turn the asymmetric DNA-NP binding potential on and off with a time period of τ_{on} and τ_{off}.

machinery walking along a cytoskeleton (*26*). Inspired by biological motors, artificial molecular machines that can move along a predefined track (*27*, *28*) have recently been developed. It has been shown that an interlocking macrocycle can be transported directionally through a cyclic track (*29*), while DNA walkers (*30*–*33*) and small synthetic molecules (*34*, *35*) can walk processively along their tracks, suggesting the possibility of achieving molecule-scale cargo transport along a designated path. However, it is nontrivial to achieve directional and processive motion in the design of the track and walker in these artificial machines. In addition, realization has only been verified along short molecular tracks. In contrast, the design of the flexibility-based DNA ratchet presented in this work is much simpler (by the synthesis of dsDNA containing the base pairs with varying degrees of l_p'). Processive and directional motion can be achieved simply by changing salt concentrations of a solution without needing different sets of DNA fuel solutions. In addition, the transport distance can be easily extended to several hundreds or thousands of nanometers by synthesizing a dsDNA molecule with repeated sequences of flexibility gradient.

RESULTS

A dsDNA fragment with flexibility gradient

A dsDNA fragment with a flexibility gradient is modeled by a semiflexible polymer chain with 64 monomers and by mixing two types of monomers with different local persistence lengths of 40 and 51 nm, as shown in Fig. 1A. A single dsDNA monomer with a diameter of 2 nm and a charge of −12 coarsely models a group of 6 base pairs. These monomers with l_p' of 40 and 51 nm mimic more flexible and less flexible groups of 6 base pairs, for instance, those with AT and GC repeats, respectively (*24*). In our model, the value of l_p' is determined by harmonic restraint applied to an angle formed by a triple of consecutive monomers. Each monomer with a given l_p' in Fig. 1A depicts the monomer in the middle of the triple with a harmonic restraint consistent with the given l_p'. The flexibility gradient is constructed from one end (least flexible, abundant with monomers with l_p' = 51 nm) to the other end (most flexible, abundant with monomers with l_p' = 40 nm) by varying the fraction of the two types of monomers, as shown in the figure. A positively charged NP is modeled by a sphere with a diameter of 4 nm and a charge of +64. The size is chosen such that the NP is wrapped around 1.6 to 1.7 turns by dsDNA at a physiological salt concentration of 0.15 M, as shown in the inset of Fig. 1B. In such case, the DNA-NP binding conformation fluctuates during BD simulations, and the NP is able to slide randomly along the dsDNA with uniform flexibility (*25*, *36*). For much larger NPs, dsDNA is adsorbed in a disordered

fashion onto the surface of the NPs, while NPs of smaller sizes are locally collected on dsDNA (*37*). For both cases, NP sliding along dsDNA is prevented.

Although the effect of flexibility variation on the dsDNA structure itself is not very notable, it becomes significant when negatively charged dsDNA fragment interacts with a highly charged cationic NP. At a physiological salt concentration of 0.15 M, an NP is wrapped around by 16 to 17 dsDNA monomers, as shown in the inset of Fig. 1B. This requires a large degree of dsDNA bending. Therefore, the free energy of DNA-NP binding is significantly influenced by dsDNA bending of sequences with different l'_p: lower for l'_p = 40 nm and higher for larger l'_p = 51 nm. As a result, the bending energy decreases with increasing flexibility along the dsDNA fragment with flexibility gradient, as shown in Fig. 1B. In the figure, bending energy is calculated for a representative DNA-NP conformation shown in the inset along the dsDNA fragment with flexibility gradient. The monomer number in the *x* axis represents the identity of the first monomer in the DNA-NP conformation. Because of a gradual decrease in bending energy, the NP wrapped around by dsDNA slides along the dsDNA fragment in the direction toward a more flexible region. Figure 3 presents the probability of the final location of an NP on a 64-mer dsDNA fragment with flexible gradient after 200 independent sets of BD simulations of a randomly located NP for each duration of $10^4\tau_{BD}$. Here, τ_{BD} is the unit of simulation time defined as σ^2/D_0, where σ is the diameter of a DNA monomer of 2 nm and D_0 is the diffusion coefficient of a single dsDNA monomer. τ_{BD} is roughly the time needed for a dsDNA monomer to move a distance equal to its own size. This figure shows that the NP slides directionally along the dsDNA fragment with flexibility gradient and that it is localized in more flexible dsDNA regions with minimum bending energy at a salt concentration of 0.15 M.

Unlike DNA-NP binding at 0.15 M (with 16 to 17 dsDNA monomers wrapping around an NP), electrostatic interaction between dsDNA and an NP is significantly weakened at an increased salt concentration of 0.81 M because of the screening effect of electrostatic interactions, and an NP is bound only with five to six dsDNA monomers. Less DNA binding leads to less dependence of dsDNA bending energy on flexibility, as shown in Fig. 1B, at a salt concentration of 0.81 M. In this case, the NP diffuses almost randomly in either direction on the dsDNA fragment because of negligible dependence of bending energy on the flexibility of dsDNA fragment.

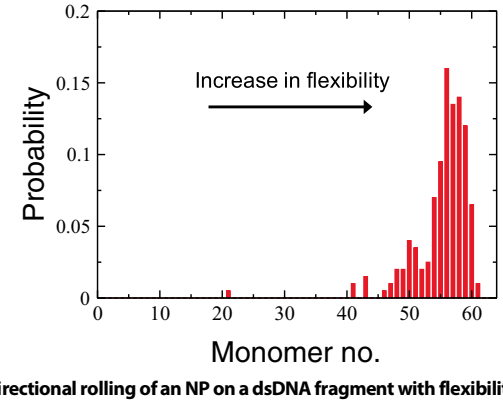

Fig. 3. Directional rolling of an NP on a dsDNA fragment with flexibility gradient. Probability of the final location of an NP on a dsDNA fragment with flexibility gradient at C_{on} = 0.15 M after BD simulations for a duration of $\tau_{on} = 10^4\tau_{BD}$, obtained from 200 independent simulations. The monomer number in the *x* axis represents the identity of the DNA monomer in the middle among those wrapping around an NP at a salt concentration of 0.15 M. Initial location of an NP was random on a dsDNA fragment at the beginning of the 200 simulations.

Directional transport of an NP along a long dsDNA with repetitive sequences of flexibility gradient

At a salt concentration of 0.15 M, an NP bound to a dsDNA fragment with flexibility gradient slides directionally toward a more flexible region of the fragment subject to asymmetric bending energy. However, the distance of directional NP transport is limited by synthetic availability of the dsDNA fragment with a flexibility gradient in a desired length that can be prepared by combining DNA base pairs with different l'_p in a sequence. Here, we propose that even farther directional transport of bound NPs can be achieved at a macroscopic length scale by a Brownian ratchet process along a long dsDNA with repeated sequences of the same flexibility gradient.

Figure 2 (A and B) shows a long dsDNA with four repeat fragments of flexibility gradient at salt concentrations of 0.15 and 0.81 M. The binding energy between the dsDNA and an NP at a salt concentration of 0.15 M is asymmetric in each repeat fragment but periodic along the entire dsDNA, as shown in Fig. 2A. On the other hand, the variation of DNA-NP binding energy along the dsDNA becomes negligible at 0.81 M, as shown in Fig. 2B. Since asymmetry in DNA-NP binding energy is on and off at salt concentrations of 0.15 and 0.81 M, salt concentrations are hereafter referred to as C_{on} and C_{off}, respectively. It is mentioned that the simulations are performed for a single repeat fragment. The presence of several repeat fragments is mimicked by using periodic boundary condition (PBC) connecting one end of the single fragment to the other end of its periodically imposed replica. This PBC is typically used in molecular simulations to mimic the macroscopic system by simulations of a nanoscale system.

Directional and processive motion of an NP bound to a long dsDNA is achieved by changing the salt concentration between C_{on} and C_{off}, as shown in Fig. 2C. When an NP is bound to a specific repeat fragment at C_{on}, the NP is wrapped around by 16 to 17 dsDNA monomers and directed to the minimum of asymmetric DNA-NP binding energy within the repeat fragment during BD simulations for a duration of τ_{ON}. As shown in Fig. 3, the simulation duration of $\tau_{ON} = 10^4\tau_{BD}$ is enough for localized distribution of NP near more flexible regions within the repeat fragment with flexibility gradient. When the salt concentration is suddenly increased to C_{off}, however, the wrapping of the NP by dsDNA is released, and the NP is bound only by five to six dsDNA monomers. The NP then diffuses randomly in either direction on dsDNA, regardless of flexibility variation, during BD simulations for a duration of τ_{off}. Since the starting location of the diffusing NP (determined by the minimum of the asymmetric binding energy at C_{on}) is biased asymmetrically toward the more flexible side of the repeat fragment, the random diffusion of the NP after τ_{off} at C_{off} results in a Gaussian distribution of the NP location spanning largely on the original repeat fragment and partially on the next repeat fragment close to the minimum of the original repeat fragment. Therefore, a non-negligible fraction of NPs initially bound to a more flexible region of the original repeat fragment can be found on the next repeat fragment after τ_{off}. When the salt concentration is reduced again to C_{on}, those that remained on the original repeat fragment during random diffusion are subjected to asymmetric binding energy along the original repeat fragment and directed again to the minimum of the binding energy. However, those that moved onto the next repeat fragment are subjected to the asymmetric binding energy of the new repeat fragment and directed to its minimum, resulting in a net forward movement by the length of the repeat fragment.

This is the mechanism of the on-off Brownian ratchet (*1*–*4*) that has been applied to several experimental systems (*5*–*7*, *13*). The success of the on-off Brownian ratchet depends on the time interval τ_{off}, during which the asymmetric potential is turned off and a Brownian particle diffuses randomly in either direction. If τ_{off} is too short, most Brownian particles remain within the boundary of the original asymmetric potential. Then, they are located to its minimum when the potential is turned on. Therefore, the net movement to the forward direction is negligible. If τ_{off} is too large, some Brownian particles can diffuse to the asymmetric potentials in the backward direction as well as to those in the forward direction. As a result, the net movement to the forward is canceled out by that to the backward. Appropriate choice of τ_{off} can lead to efficient directional transport of the Brownian particles.

Therefore, we investigated the effect of different τ_{off} on random diffusion of an NP at C_{off}, as shown in Fig. 4. For an NP initially located at the most flexible region of an original dsDNA repeat fragment (more specifically, we consider an NP on the 60th dsDNA monomer of an original 64-monomer repeat fragment), BD simulations were performed at C_{off} for durations between $\tau_{off} = 5 \times 10^2 \tau_{BD}$ and $10^4 \tau_{BD}$. The probability data in Fig. 4 were obtained from 300 independent simulations at each τ_{off}. Figure 4A shows the probability of the final location of an NP after each simulation duration of $\tau_{off} = 5 \times 10^2 \tau_{BD}$, $10^3 \tau_{BD}$, and $5 \times 10^3 \tau_{BD}$. In the figure, dsDNA monomers in the original repeat fragment are numbered from 1 to 64 with increasing flexibility (light orange–colored shades in the figure). The numbers of the dsDNA monomers in other repeat fragments in the forward direction increase sequentially from 65, whereas those in the backward direction decrease from 0 down to negative numbers. Figure 4B shows the probability of an NP in the original repeat fragment to jump to other repeat fragments. Separation of the final repeat fragment from the original repeat fragment is denoted by ΔN_{jump}. Positive values of ΔN_{jump} imply net NP displacement in the forward direction, whereas negative values imply net displacement in the backward direction.

In Fig. 4, simulations performed for the duration of $\tau_{off} = 5 \times 10^2 \tau_{BD}$ resulted in nonzero probability data spanning only on the original repeat fragment ($\Delta N_{jump} = 0$) and the next repeat fragment in the forward direction ($\Delta N_{jump} = 1$). Probabilities of an NP for $\Delta N_{jump} = 0$ and 1 are 0.81 and 0.19, respectively, implying that when the asymmetric potential is turned on at C_{on}, 19% of NPs move forward to the minimum of the next repeat fragment, while the other 81% of NPs remain on the original repeat fragment at the potential minimum. On the other hand, after a longer simulation duration of $\tau_{off} \geq 10^3 \tau_{BD}$, not only there were more NPs diffusing in the forward direction ($\Delta N_{jump} \geq 1$) but also a fraction of NPs were also found in the repeat fragment in the backward direction ($\Delta N_{jump} \leq -1$). More specifically, at $\tau_{off} = 5 \times 10^3 \tau_{BD}$, 32% of NPs were found on the repeat fragments in the forward direction ($\Delta N_{jump} = 1$, 2, and 3), and 20% of NPs were found in the backward direction ($\Delta N_{jump} = -1$ and -2). In such cases, the net NP displacement in the forward direction is canceled to some degree by that in the backward direction. Thus, the Brownian ratchet process is not very efficient. It is noted that the probability data in Fig. 4A were not very symmetric as expected for a Brownian particle performing random diffusion. This implies that the asymmetric potential in the DNA-NP binding energy is not completely off even at C_{off}. For simplicity, we will continue to say that the asymmetric potential is off at C_{off}, neglecting the weak asymmetry at this salt concentration.

Simple prediction of the efficiency of the Brownian ratchet process can be made on the basis of probabilities of NP displacement in forward and backward directions at C_{off}. Figure 4C shows the difference between forward and backward probabilities, $P_f - P_b$, at different τ_{off} calculated on the basis of probability data shown in Fig. 4B. P_f is the sum of probabilities in the forward direction with $\Delta N_{jump} \geq 1$, and P_b is the sum of those in the backward direction with $\Delta N_{jump} \leq -1$. The larger $P_f - P_b$ is, the more chance of NPs moving in the forward direction at C_{on}. As shown in Fig. 4C, it was found that there was an optimal duration, which was at $\tau_{off} = 10^3 \tau_{BD}$, for efficient Brownian ratchet process with a maximum $P_f - P_b$ of 0.22.

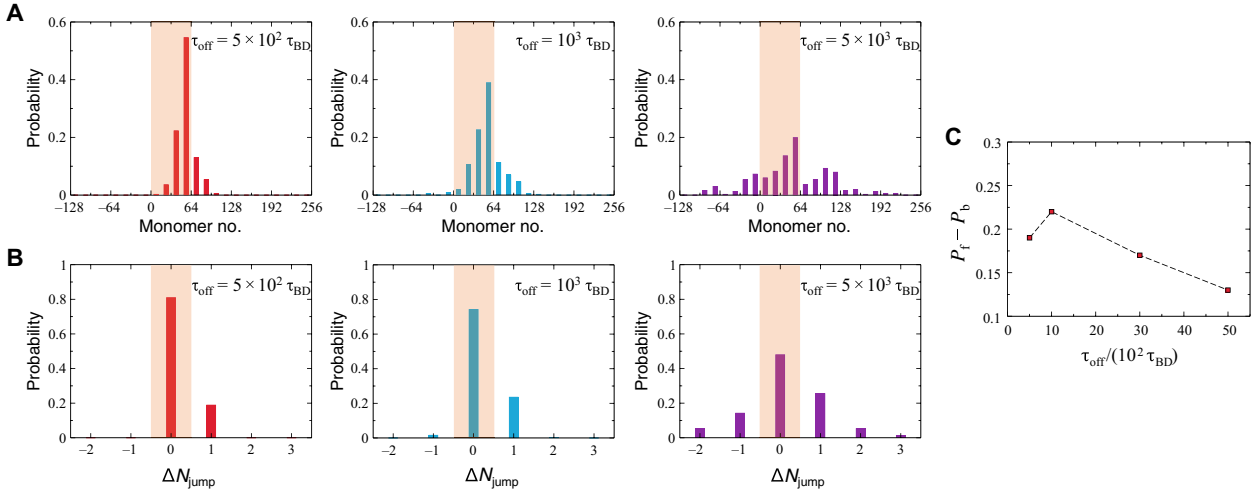

Fig. 4. Brownian motion of an NP at C_{off} = 0.81 M. (**A**) Probability of final location of an NP initially bound to the 60th monomer (most flexible region of the first repeat fragment) after each simulation duration of $\tau_{off} = 5 \times 10^2 \tau_{BD}$, $10^3 \tau_{BD}$, and $5 \times 10^3 \tau_{BD}$, calculated with a bin size of 16. (**B**) Probability of NP jump from the original repeat fragment to the other repeat fragments, ΔN_{jump}, after τ_{off}. ΔN_{jump} is positive for forward direction and negative for backward direction. Light orange–colored shades indicate the original repeat fragment. These histogram data in the figures were obtained from 300 independent simulations at each τ_{off}. (**C**) Probability of net directional motion of an NP in the forward direction ($P_f - P_b$) estimated by the difference between probabilities for forward (P_f) and backward (P_b) diffusion of an NP after τ_{off}.

To prove the realization of this flexibility-based DNA Brownian ratchet process for directional NP transport, we performed BD simulations repetitively at C_{on} and C_{off}, with a fixed duration of $\tau_{on} = 10^4\tau_{BD}$ and different durations of τ_{off}. A total of 40 cycles of on-off simulations were performed at C_{on} and C_{off} for $\tau_{off} = 5 \times 10^2\tau_{BD}$ and $10^3\tau_{BD}$, and 20 cycles of on-off simulations were performed for $\tau_{off} = 5 \times 10^3\tau_{BD}$ and $10^4\tau_{BD}$. For each τ_{off}, we performed 20 independent sets of these cyclic simulations to obtain the average net displacement.

Figure 5A shows the trajectories of 20 independent simulations for $\tau_{off} = 10^3\tau_{BD}$. The *x* axis represents the simulation time over cycles of BD simulations at C_{on} and C_{off}, while the *y* axis represents ΔN_{jump}, which is the repeat fragment to which an NP belongs at each time relative to the starting repeat fragment. In the figure, flat regions are observed, with occasional transitions between different values of ΔN_{jump}. Flat regions with constant ΔN_{jump} were obtained during simulations at C_{on}, while regions with sharp transitions were during simulations at C_{off}. Flat regions are often prolonged since the random diffusion at C_{off} does not lead to NP jump to another repeat fragment.

Figure 5B shows the average of 20 independent simulations at each τ_{off}. As predicted above on the basis of $P_f - P_b$, the net NP transport was the most efficient for $\tau_{off} = 10^3\tau_{BD}$. After 40 cycles of simulations at C_{on} and C_{off}, an NP is transported through three DNA repeat fragments away from the original repeat fragment. This shows that the flexibility-based DNA Brownian ratchet proposed in this work can be realized by repetitively changing salt concentrations between C_{on} and C_{off}.

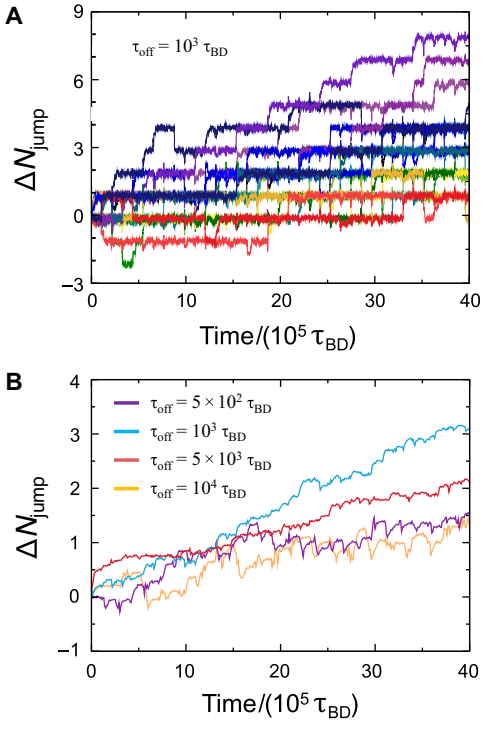

Fig. 5. Simulation results of directional motion of an NP in the forward direction. (**A**) Net displacement of an NP with time starting from an original repeat fragment and arriving at a repeat fragment separated by ΔN_{jump} fragments, presented for all 20 independent simulation sets with 40 repeated changes between salt concentrations of C_{on} and C_{off} with simulation durations of $\tau_{on} = 10^4\tau_{BD}$ and $\tau_{off} = 10^3\tau_{BD}$. (**B**) Net displacement averaged over the 20 independent simulation sets for different simulation durations of $\tau_{off} = 5 \times 10^2\tau_{BD}$, $10^3\tau_{BD}$, $5 \times 10^3\tau_{BD}$, and $10^4\tau_{BD}$. In each simulation set, the asymmetric potential is turned on and off repeatedly 20 times for $\tau_{off} = 5 \times 10^3\tau_{BD}$ and $10^4\tau_{BD}$ and 40 times for $\tau_{off} = 5 \times 10^2\tau_{BD}$ and $10^3\tau_{BD}$. Positive values for ΔN_{jump} indicates net displacement in the forward direction.

Stability of DNA-NP binding and NP diffusion under external force field

For successful realization of this proposed Brownian ratchet, periodic and repetitive change in the solution salt concentration is critical. One possibility lies in the use of a microfluidic device in which two solutions with different salt concentrations of C_{on} and C_{off} are alternatively injected (*38*, *39*). Although these alternating-injection microfluidic devices were developed to enhance the mixing efficiency in microfluidic channels, it is possible that the alternating injection of two salt solutions with different concentrations can be used for the periodic and repetitive change in the solution salt concentration required for the Brownian ratchet device proposed in this work. However, the flow of injected solutions in a microfluidic device exerts hydrodynamic drag forces on DNA and an NP, possibly influencing the stability of DNA-NP binding and diffusion of an NP on DNA. Therefore, we performed additional simulations under uniform force field that coarsely mimics hydrodynamic drag forces exerted by the laminar flow in a microfluidic channel. As a representative model system, the binding complex of an NP and a dsDNA with four repeat fragments (containing 256 dsDNA monomers) was simulated under constant, uniform force field in the subpiconewton range (see fig. S1). Two ends of the dsDNA are anchored at a separation of 230σ less than its fully stretched contour length, 256σ, to allow for DNA wrapping around an NP at the salt concentration of 0.15 M. Constant forces are applied to all DNA monomers in the direction perpendicular to the DNA. A twice stronger force is applied to an NP in the same direction because the hydrodynamic drag force increases with the size of an object.

Simulation results show that the wrapping structure of DNA around an NP at the salt concentration of $C_{on} = 0.15$ M remains stable up to the force of 0.20 pN applied to an NP, as shown in Fig. 6A. At applied forces exceeding 0.20 pN, the DNA wrapping around an NP is disrupted (Fig. 6A), weakening the asymmetry in DNA-NP binding because of the relaxation of sharply bent DNA monomers from the wrapping structure. In the range of weak external forces (≤ 0.20 pN), an NP wrapped around by DNA at C_{on} is kept localized at the minimum of the asymmetric potential in each DNA fragment with flexibility gradient during simulation duration of $\tau_{ON} = 10^4\tau_{BD}$. At the salt concentration of $C_{off} = 0.81$ M, the binding of an NP on DNA remains stable at applied forces of 0.60 pN or less, whereas at stronger applied forces, an NP comes off from DNA. In the range of weak external forces (≤ 0.60 pN), an NP at C_{off} performs random Brownian motion on DNA because the asymmetric potential is off, as in the case of no external force. These results set the upper bound of external forces of 0.20 pN under which the proposed DNA-based Brownian ratchet can work. Under external forces exceeding 0.20 pN, the directional motion of an NP at C_{on} along the flexibility gradient is ineffective because of the disruption of the wrapping structure of DNA-NP binding, while the random Brownian motion of an NP at C_{off} is less affected by the external force of 0.60 pN or less. Figure 6B presents the probability of the final location of an NP at the applied force of 0.20 pN after simulation duration of $\tau_{off} = 10^3\tau_{BD}$ at C_{off}, and the near symmetry in the probability distribution around a starting location, set to zero, proves the random Brownian motion of an NP at C_{off} (also in fig. S2). In summary, the flexibility-biased localization of an NP at C_{on} and the random Brownian motion at C_{off} are observed even in the presence of external uniform forces of

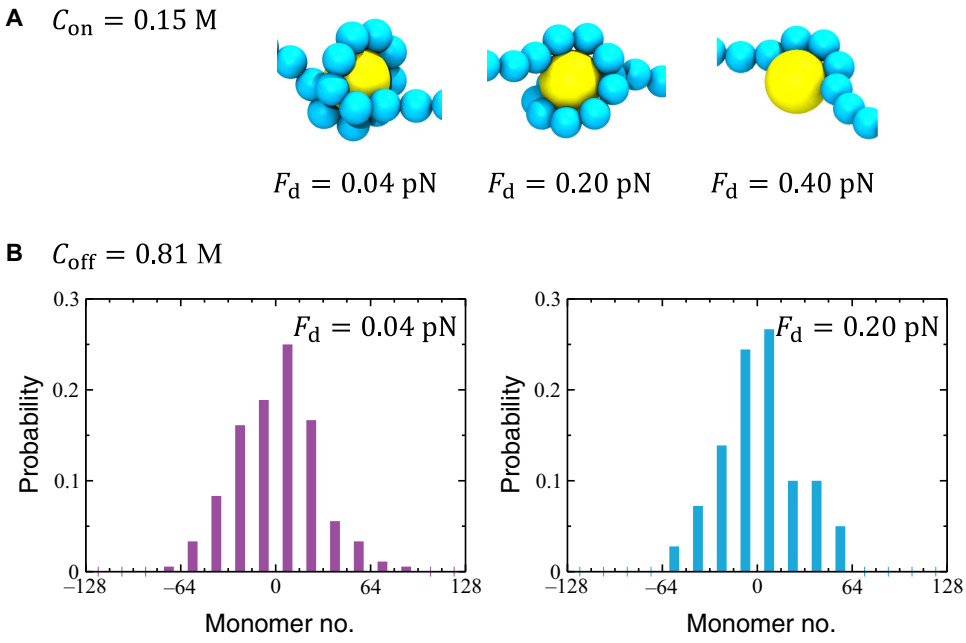

Fig. 6. DNA-NP under constant force field. (**A**) Snapshots of an NP with DNA at C_{on} = 0.15 M subject to external forces, F_d, of 0.04, 0.20, and 0.40 pN. (**B**) Probability of final location of an NP at C_{off} = 0.81 M after BD simulations of $\tau_{off} = 10^3\tau_{BD}$ under external forces F_d = 0. 04 and 0.20 pN. An NP is initially bound to the most flexible region of a flexibility gradient, and this initial location is set to the monomer number of zero in the figures. The probability distributions in (B) are obtained from 180 independent simulations.

0.20 pN or less, ensuring the success of the proposed Brownian ratchet device under weak external force.

DISCUSSION

We proposed a DNA-based Brownian ratchet system for directional transport of a positively charged NP and proved its realization by BD simulations. Outstanding advantages of this system over earlier Brownian ratchet devices are that nanometer-scale Brownian particles can be transported in a specific direction by using strong electrostatic interactions between NPs and dsDNA and that the NP delivery follows the path along a single, long, dsDNA molecule, adding spatial precision for NP transport. Although we performed simulations only for a single NP transported along dsDNA, several NPs could be collected on the long dsDNA and processively transported toward the end of the dsDNA. Once NPs are collected at one end, they can be released by increasing salt concentration further above C_{off}. Such highly localized collection of NPs can be useful in many applications.

Although several molecule-scale walkers have been developed in recent years (*27*, *28*, *30*–*35*), the design of walker and track is nontrivial for processive and directional movements. On the contrary, the construction of the DNA Brownian ratchet proposed in this work is simpler. It only requires the design of a track with proper flexibility variation. Directional and processive transport of NPs can be achieved only by changing salt concentrations without needing alternative fuel solutions with different DNA strands. Last, the transport distance for NPs can be easily extended by duplicating the same DNA sequence with a flexibility gradient. Functionalization of NPs may extend the utility of the present DNA Brownian ratchet for transport of other functional groups attached onto NPs.

The sequence-dependent flexibility of a dsDNA has rarely been used as a tool for manipulating DNA-incorporated nanostructures. In our Brownian ratchet system, the asymmetric potential in each dsDNA fragment is built by aligning DNA base pairs with gradual flexibility variation. Although variation of dsDNA flexibility is not significant in structure determination of the dsDNA itself, the effect is augmented when it binds with highly charged cationic NPs, which requires a large degree of dsDNA bending. Therefore, one can find the utility of this flexibility-based NP control in the development of nanocomposites containing dsDNA and NPs.

Last, repetitive change in the solution salt concentration may induce hydrodynamic drag forces on DNA and NP by the flow during alternate injection of two solutions with different concentrations. It was shown from BD simulations under applied forces that the binding complex of DNA and NP remains stable, and the diffusion of an NP on DNA is not significantly influenced in the subpiconewton range of applied forces. Therefore, the realization of the proposed DNA-based Brownian ratchet relies on the development of a microfluidic device in which two solutions with different concentrations are injected alternately and the resultant hydrodynamic drag forces on nanometer-scale objects are in the subpiconewton range.

MATERIALS AND METHODS

Models of a dsDNA and an NP

As a model of a long dsDNA molecule, we used a semiflexible polymer chain. Each monomer had a diameter of 2 nm and a charge of −12, coarsely mimicking a group of 6 DNA base pairs. The charge per base pair was −2 at physiological pH, and a rise per base pair was 0.34 nm in B-DNA. An NP was modeled by a spherical particle with a diameter of 4 nm and a charge of +64. The size and charge of an NP were chosen such that the NP was wrapped around 1.6 to 1.7 turns by dsDNA at a physiological salt concentration of 0.15 M (*25*). In this case, conformational fluctuations of the DNA-NP binding complex enabled random sliding along dsDNA with uniform flexibility (*25*, *36*).

The bonded interaction between a pair of DNA monomers was modeled by a combination of finite extension nonlinear elastic (FENE) potential energy

$$U_b(r) = -\frac{1}{2}k_b R_b^2 \ln[1-(r/R_b)^2] \quad (1)$$

and a repulsive part of Lennard-Jones (LJ) potential energy

$$U_r(r) = \begin{cases} 4\varepsilon_{LJ}\left[\left(\frac{\sigma}{r}\right)^{12} - \left(\frac{\sigma}{r}\right)^{6}\right] + \varepsilon_{LJ}, & 0 < r < 2^{1/6}\sigma \\ 0 & , \quad \text{elsewhere} \end{cases} \quad (2)$$

where r is the distance between a pair of consecutive DNA monomers, $k_b = 30k_BT/\sigma^2$, $R_b = 1.5\sigma$, σ is the diameter of DNA monomers of 2 nm, and $\varepsilon_{LJ} = 1k_BT$ with the Boltzmann constant k_B and the temperature T. The parameters for FENE potential energy were chosen to prevent bond crossing. Local flexibility of dsDNA was modeled by harmonic restraint applied to the angle formed by a triple of consecutive DNA monomers, i, $i+1$, and $i+2$, as

$$U_\theta(\theta) = \frac{k_\theta}{2}\theta^2 \quad (3)$$

where θ is the angle between two consecutive bond vectors $\vec{b}_{i,i+1}$ and $\vec{b}_{i+1,i+2}$ of monomers i, $i+1$, and $i+2$. Here, a parameter k_θ determines local persistence length of a triple of DNA monomers. The variation of local persistence length of dsDNA ranges from 40 to 55 nm, which was reported in the work of Geggier and Vologodskii (*23*). We used $k_\theta = 18k_BT/\text{rad}^2$ and $24k_BT/\text{rad}^2$ to represent more flexible and less flexible triples with local persistence lengths of 40 and 51 nm, respectively, as calculated in our previous work (*25*). The local persistence length of each triple is specified in Fig. 1A labeled for the monomer in the middle by l_p' of either 40 or 51 nm.

Nonbonded interactions were modeled by a combination of excluded volume interactions and electrostatic interactions. Excluded volume interactions between a pair of nonbonded DNA monomers and between an NP and DNA monomers were described by repulsive LJ potential energy identical to Eq. 2 above, but with a shift of r_0 to describe size difference between an NP and DNA monomers

$$U_r(r) = \begin{cases} 4\varepsilon_{LJ}\left[\left(\frac{\sigma}{r-r_0}\right)^{12} - \left(\frac{\sigma}{r-r_0}\right)^{6}\right] + \varepsilon_{LJ}, & 0 < r-r_0 < 2^{1/6}\sigma \\ 0 & , \quad \text{elsewhere} \end{cases} \quad (4)$$

Here, r_0 was 0 for a pair of DNA monomers, but 0.5σ for a pair of a DNA monomer and an NP because the size of an NP was twice that of DNA monomers. On the other hand, the linearized Debye-Hückel potential energy in Eq. 5 described electrostatic interactions between a pair of DNA monomers and between an NP and DNA monomers

$$U_{DH} = \frac{l_B z_i z_j k_B T}{(1+\kappa\sigma_i/2)(1+\kappa\sigma_j/2)} \frac{\exp\left[-\kappa\left(r-(\sigma_i+\sigma_j)/2\right)\right]}{r} \quad (5)$$

where z_i and z_j are the charges of particles i and j, while σ_i and σ_j are the diameters of particles. l_B is the Bjerrum length defined as $e^2/(4\pi\varepsilon_0\varepsilon_r k_B T) \approx 0.71$ nm in pure water at 298 K, in which e, ε_0, and ε_r are elementary charge, vacuum permittivity, and relative dielectric constant in pure water, respectively. The inverse Debye length κ is given by $\kappa \approx (8\pi l_B N_A C_{salt})^{1/2}$, where N_A is the Avogadro's number. It is adjusted by the concentration of monovalent salt C_{salt}. In this work, salt concentrations were changed between $C_{salt} = 0.15$ and 0.81 M corresponding to $\kappa^{-1} = 0.80$ and 0.34 nm, respectively.

Use of PBC for a dsDNA with repetitive flexibility gradient

In this work, the construction of a periodic and asymmetric potential along a long dsDNA molecule was critical for directional and processive transport of an NP bound to the dsDNA. For this purpose, a long dsDNA molecule was composed of several repeating fragments of 64 monomers (corresponding to 384 base pairs) as shown in Fig. 2A, each of which had a flexibility gradient. The flexibility gradient was constructed by varying the fraction of monomers with $l_p' = 40$ and 51 nm along the repeat fragment, as shown in Fig. 1A, with increasing flexibility as the fraction of monomers with $l_p' = 40$ nm increased from left to right in the fragment.

Technically, however, only a single repeat fragment was explicitly considered in BD simulations with the use of PBC, in which one end of the repeat fragment was connected to the other end of its periodically imposed replica. Therefore, when an NP bound to one end of the repeat fragment moved to the other end across the simulation box, it was interpreted as a jump from the repeat fragment to the next nearest fragment represented as its periodic replica. The use of PBC to mimic a series of the repeat fragments with flexibility gradient is reasonable because the repeat fragment of 64 monomers had a contour length of 130 nm, much longer than the persistence length of our dsDNA model (between 40 and 51 nm in case of mixed monomers with different l_p'). The simulation box had a longitudinal dimension of 50σ, along which the PBC was applied. The dynamics of a single NP was investigated in the system.

BD simulation method

We performed BD simulations with a simulation package, GROMACS v. 4.5.4. BD simulations can simulate stochastic displacements of an NP and DNA monomers through a position Langevin equation, as shown below in Eq. 6, instead of explicitly incorporating solvent molecules into the system. Electrostatic screening by the presence of monovalent ions was implicitly taken into account by using Debye-Hückel potential energy in Eq. 5 instead of their explicit presence. Hydrodynamic interactions between DNA monomers and between a DNA monomer and an NP were not considered in this work. Hydrodynamic interactions are known to influence the diffusion of NPs quantitatively, particularly under strongly confined environment (*40*). However, the qualitative conclusion in this work that the Brownian ratchet device can be realized by repetitively combining the flexibility-biased NP diffusion at C_{on} and the random, unbiased diffusion at C_{off} does not seem largely influenced by the quantitative change in NP diffusion.

Given a position of a particle at time t, the updated position at the next time step of $t + \Delta t$ is determined by

$$\mathbf{r}(t+\Delta t) = \mathbf{r}(t) + \frac{D\mathbf{F}(t)}{k_B T}\Delta t + \mathbf{R}(\Delta t) \quad (6)$$

Here, $\mathbf{F}(t)$ is the total force acting on the particle, D is the diffusion coefficient of each particle in dilute solution, and $\mathbf{R}(\Delta t)$ is a random

displacement with a Gaussian distribution function with zero mean and variance of $6D\Delta t$. The diffusion coefficient of an NP was half of that of DNA monomers (referred to as D_0) because of size difference. The unit time of BD simulations was set by $\tau_{BD} = \sigma^2/D_0$ using a dsDNA monomer as a reference, which was roughly the average time for a DNA monomer to move a distance of its own size σ. A time step $\Delta t = 10^{-4}\tau_{BD}$ was used for all simulations.

Main results shown in Fig. 5 were obtained by cycles of BD simulations at C_{on} = 0.15M and C_{off} = 0.81 M. Each simulation at C_{on} = 0.15 M was performed for a fixed duration of 10^8 time steps, or $\tau_{on} = 10^4\tau_{BD}$. On the other hand, simulations at C_{off} = 0.81 M were performed for durations between 5×10^6($\tau_{off} = 5 \times 10^2\tau_{BD}$) and 10^8 time steps ($\tau_{off} = 10^4\tau_{BD}$), as mentioned in relevant parts of the main text. Statistical properties reported in this work were calculated by averaging several tens of independent simulations. This was mentioned in the main text when we discussed the data presented in Figs. 3 to 5.

The BD simulations under external forces were performed by adding an extra force to $\mathbf{F}(t)$ in Eq. 6. Constant forces were applied to all DNA monomers, and a twice stronger force was applied to an NP, all in the same direction perpendicular to DNA as shown in fig. S1. The application of a twice stronger force to an NP than that to DNA was based on the Stokes' formula saying that the hydrodynamic drag force is proportional to the size of an object. Forces of 0.02, 0.10, and 0.20 (in the unit of k_BT/σ) were applied to an NP, and half the forces were applied to DNA. The applied forces were converted to 0.04, 0.20, and 0.40 pN at a temperature of 300 K.

SUPPLEMENTARY MATERIALS

Supplementary material for this article is available at http://advances.sciencemag.org/cgi/content/full/5/4/eaav4943/DC1

Fig. S1. Simulation model systems of DNA-NP binding at C_{on} = 0.15 M under external force.

Fig. S2. Probability distribution of an NP at C_{off} = 0.81 M after Brownian motion for a duration of $\tau_{off} = 10^3\tau_{BD}$ under external force.

REFERENCES AND NOTES

1. R. D. Astumian, Thermodynamics and kinetics of a Brownian motor. *Science* **276**, 917–922 (1997).
2. P. Reimann, Brownian motors: Noisy transport far from equilibrium. *Phys. Rep.* **361**, 57–265 (2002).
3. P. Hänggi, F. Marchesoni, Artificial Brownian motors: Controlling transport on the nanoscale. *Rev. Mod. Phys.* **81**, 387–442 (2009).
4. S. Erbas-Cakmak, D. A. Leigh, C. T. McTernan, A. L. Nussbaumer, Artificial molecular machines. *Chem. Rev.* **115**, 10081–10206 (2015).
5. J. Rousselet, L. Salome, A. Ajdari, J. Prost, Directional motion of Brownian particles induced by a periodic asymmetric potential. *Nature* **370**, 446–448 (1994).
6. L. P. Faucheux, L. S. Bourdieu, P. D. Kaplan, A. J. Libchaber, Optical thermal ratchet. *Phys. Rev. Lett.* **74**, 1504–1507 (1995).
7. J. S. Bader, R. W. Hammond, S. A. Henck, M. W. Deem, G. A. McDermott, J. M. Bustillo, J. W. Simpson, G. T. Mulhern, J. M. Rothberg, DNA transport by a micromachined Brownian ratchet device. *Proc. Natl. Acad. Sci. U.S.A.* **96**, 13165–13169 (1999).
8. C. Marquet, A. Buguin, L. Talini, P. Silberzan, Rectified motion of colloids in asymmetrically structured channels. *Phys. Rev. Lett.* **88**, 168301 (2002).
9. S. Matthias, F. Müller, Asymmetric pores in a silicon membrane acting as massively parallel brownian ratchets. *Nature* **424**, 53–57 (2003).
10. S.-H. Lee, K. Ladavac, M. Polin, D. G. Grier, Observation of flux reversal in a symmetric optical thermal ratchet. *Phys. Rev. Lett.* **94**, 110601 (2005).
11. L. Bogunovic, R. Eichhorn, J. Regtmeier, D. Anselmetti, P. Reimann, Particle sorting by a structured microfluidic ratchet device with tunable selectivity: Theory and experiment. *Soft Matter* **8**, 3900–3907 (2012).
12. D. Reguera, A. Luque, P. S. Burada, G. Schmid, J. M. Rubí, P. Hänggi, Entropic splitter for particle separation. *Phys. Rev. Lett.* **108**, 020604 (2012).
13. S.-H. Wu, N. Huang, E. Jaquay, M. L. Povindelli, Near-field, on-chip optical Brownian ratchets. *Nano Lett.* **16**, 5261–5266 (2016).
14. M. J. Skaug, C. Schwemmer, S. Fringes, C. D. Rawlings, A. W. Knoll, Nanofluidic rocking Brownian motors. *Science* **359**, 1505–1508 (2018).
15. E. Braun, Y. Eichen, U. Sivan, G. Ben-Yoseph, DNA-templated assembly and electrode attachment of a conducting silver wire. *Nature* **391**, 775–778 (1998).
16. S. Kosuri, G. M. Church, Large-scale de novo DNA Synthesis: Technologies and applications. *Nat. Methods* **11**, 499–507 (2014).
17. P. W. K. Rothemund, Folding DNA to create nanoscale shapes and patterns. *Nature* **440**, 297–302 (2006).
18. N. C. Seeman, H. F. Sleiman, DNA nanotechnology. *Nat. Rev. Mater.* **3**, 17068 (2017).
19. J. D. Le, Y. Pinto, N. C. Seeman, K. Musier-Forsyth, T. A. Taton, R. A. Kiehl, DNA-templated self-assembly of metallic nanocomponent arrays on a surface. *Nano Lett.* **4**, 2343–2347 (2004).
20. B. Yurke, A. J. Turberfield, A. P. Mills Jr., F. C. Simmel, J. L. Neumann, A DNA-fuelled molecular machine made of DNA. *Nature* **406**, 605–608 (2000).
21. H. Yan, X. Zhang, Z. Shen, N. C. Seeman, A robust DNA mechanical device controlled by hybridization topology. *Nature* **415**, 62–65 (2002).
22. H. Gu, J. Chao, S.-J. Xiao, N. C. Seeman, A proximity-based programmable DNA nanoscale assembly line. *Nature* **465**, 202–205 (2010).
23. S. Geggier, A. Vologodskii, Sequence dependence of DNA bending rigidity. *Proc. Natl. Acad. Sci. U.S.A.* **107**, 15421–15426 (2010).
24. H.-M. Chuang, J. G. Reifenberger, H. Cao, K. D. Dorfman, Sequence-dependent persistence length of long DNA. *Phys. Rev. Lett.* **119**, 227802 (2017).
25. S. Park, H. Joo, J. S. Kim, Directional rolling of positively charged nanoparticles along a flexibility gradient on long DNA molecules. *Soft Matter* **14**, 817–825 (2018).
26. J. Howard, *Mechanics of Motor Proteins and the Cytoskeleton* (Sinauer Associates, Sunderland, 2001).
27. E. R. Kay, D. A. Leigh, Rise of the molecular machines. *Angew. Chem. Int. Ed.* **54**, 10080–10088 (2015).
28. J. M. Abendroth, O. S. Bushuyev, P. S. Weiss, C. J. Barrett, Controlling motion at the nanoscale: Rise of the molecular machines. *ACS Nano* **9**, 7746–7768 (2015).
29. M. R. Wilson, J. Solà, A. Carlone, S. M. Goldup, N. Lebrasseur, D. A. Leigh, An autonomous chemically fuelled small-molecule motor. *Nature* **534**, 235–240 (2016).
30. W. B. Sherman, N. C. Seeman, A precisely controlled DNA biped walking device. *Nano Lett.* **4**, 1203–1207 (2004).
31. J.-S. Shin, N. A. Pierce, A synthetic DNA walker for molecular transport. *J. Am. Chem. Soc.* **126**, 10834–10835 (2004).
32. Y. Tian, Y. He, Y. Chen, P. Yin, C. Mao, A DNAzyme that walks processively and autonomously along a one-dimensional track. *Angew. Chem. Int. Ed.* **44**, 4355–4358 (2005).
33. I. Y. Loh, J. Cheng, S. R. Tee, A. Efremov, Z. Wang, From bistate molecular switches to self-directed track-walking nanomotors. *ACS Nano* **8**, 10293–10304 (2014).
34. M. von Delius, E. M. Geertsema, D. A. Leigh, A synthetic small molecule that can walk down a track. *Nat. Chem.* **2**, 96–101 (2010).
35. M. J. Barrell, A. G. Campaña, M. von Delius, E. M. Geertsema, D. A. Leigh, Light-driven transport of a molecular walker in either direction along a molecular track. *Angew. Chem. Int. Ed.* **50**, 285–290 (2011).
36. N. Bagatella-Flores, H. Schiessel, W. M. Gelbart, Statics and dynamics of polymer-wrapped colloids. *J. Phys. Chem. B* **109**, 21305–21312 (2005).
37. A. A. Zinchenko, T. Sakaue, S. Araki, K. Yoshikawa, D. Baigl, Single-chain compaction of long duplex DNA by cationic nanoparticles: Modes of interaction and comparison with chromatin. *J. Phys. Chem. B* **111**, 3019–3031 (2007).
38. I. Glasgow, N. Aubry, Enhancement of microfluidic mixing using time pulsing. *Lab Chip* **3**, 114–120 (2003).
39. Y. K. Suh, S. Kang, A review on mixing in microfluidics. *Micromachines* **1**, 82–111 (2010).
40. X. Yang, C. Liu, Y. Li, F. Marchesnoi, P. Hänggi, H. P. Zhang, Hydrodynamic and entropic effects on colloidal diffusion in corrugated channels. *Proc. Natl. Acad. Sci. U.S.A.* **114**, 9564–9569 (2017).

Acknowledgments: We thank H. W. Cho for helpful discussions. **Funding:** This research was supported by the National Research Foundation of Korea (NRF) under grant nos. NRF-2015R1D1A1A01059005 and NRF-2018R1D1A1B07043246. **Author contributions:** J.S.K. conceived and designed this work. S.P. and J.S.K. developed the computational models. S.P. and J.S. conducted the computer simulations and data analysis. S.P. and J.S.K. wrote the manuscript. **Competing interests:** The authors declare that they have no competing interests. **Data and materials availability:** All data needed to evaluate the conclusions in the paper are present in the paper and/or the Supplementary Materials. Additional data related to this paper may be requested from the authors.

Submitted 21 September 2018
Accepted 8 February 2019
Published 5 April 2019
10.1126/sciadv.aav4943

Citation: S. Park, J. Song, J. S. Kim, In silico construction of a flexibility-based DNA Brownian ratchet for directional nanoparticle delivery. *Sci. Adv.* **5**, eaav4943 (2019).

In silico construction of a flexibility-based DNA Brownian ratchet for directional nanoparticle delivery

Suehyun Park, Jeongeun Song and Jun Soo Kim

Sci Adv **5** (4), eaav4943.
DOI: 10.1126/sciadv.aav4943